HHS Public Access

Author manuscript

Sci Signal. Author manuscript; available in PMC 2015 April 01.

Published in final edited form as:

Sci Signal. ; 8(359): ra3. doi:10.1126/scisignal.2005748.

STIM2 enhances receptor-stimulated Ca^{2+} signaling by promoting recruitment of STIM1 to the endoplasmic reticulum-plasma membrane junctions

Hwei Ling Ong[1], **Lorena Brito de Souza**[1], **Changyu Zheng**[2], **Kwong Tai Cheng**[3], **Xibao Liu**[1], **Corinne Goldsmith**[2], **Stefan Feske**[4], and **Indu S. Ambudkar**[1]

[1]Secretory Physiology Section, Molecular Physiology and Therapeutics Branch, NIDCR, NIH, MD 20892

[2]Translational Research Core, Molecular Physiology and Therapeutics Branch, NIDCR, NIH, MD 20892

[3]Department of Pharmacology, College of Medicine, University of Illinois at Chicago, Chicago, IL 60612

[4]Department of Pathology, New York University Langone Medical Center, New York, NY 10016, USA

Abstract

A central component of receptor-evoked Ca^{2+} signaling is store-operated Ca^{2+} entry (SOCE), which is activated by the assembly of STIM1-Orai1 channels in endoplasmic reticulum (ER) and plasma membrane (PM) (ER-PM) junctions in response to depletion of ER-Ca^{2+}. We report that STIM2 enhances agonist-mediated activation of SOCE by promoting STIM1 clustering in ER-PM junctions at low stimulus intensities. Targeted deletion of STIM2 in mouse salivary glands diminished fluid secretion in vivo and SOCE activation in dispersed salivary acinar cells stimulated with low concentrations of muscarinic receptor agonists. STIM2 knockdown in HEK293 cells diminished agonist-induced Ca^{2+} signaling and nuclear translocation of NFAT. STIM2 lacking five C-terminal amino acid residues did not promote formation of STIM1 puncta at low concentrations of agonist, whereas coexpression of STIM2 with STIM1 mutant lacking the polybasic region, STIM1ΔK, resulted in coclustering of both proteins. Together, our findings suggest that STIM2 recruits STIM1 to ER-PM junctions at low stimulus intensities when ER-Ca^{2+} stores are mildly depleted, thus increasing the sensitivity of Ca^{2+} signaling to agonists.

Address all correspondence to: Dr. Indu S. Ambudkar, Bldg. 10/Room 1N-113, NIDCR, NIH, Bethesda, MD 20892, USA. Phone: 301-496-5298; Fax: 301-402-1228; indu.ambudkar@nih.gov.

AUTHOR CONTRIBUTIONS

Conceived and designed the experiments: H.L.O., L.B.S. and I.S.A. Performed the experiments: H.L.O., L.B.S., X.L. and C.Z. Analyzed the data: H.L.O., L.B.S., X.L. and I.S.A.

Contributed reagents/materials/analysis tools: C.Z., K.T.C., C.G. and S.F. Wrote the paper: H.L.O. and I.S.A.

Competing interests: XXX

INTRODUCTION

Store-operated calcium entry (SOCE) is a critical mechanism that provides local and global Ca^{2+} signals, which regulate a broad range of physiological functions in many cell types. SOCE is activated in response to depletion of endoplasmic reticulum (ER)-Ca^{2+} stores. Physiologically, this is achieved as a result of agonist-stimulated inositol trisphosphate (IP_3) generation and release of ER-Ca^{2+} through the IP_3 receptor (IP_3 R). Experimental paradigms to activate SOCE include treatment of cells with blockers of the ER-Ca^{2+} pump, which result in passive leak of Ca^{2+} from the ER through as yet undefined pathway(s). SOCE is achieved primarily by the gating of the plasma membrane (PM)-localized channel, Orai1, by the ER-localized Ca^{2+}-sensing protein, STIM1 (1-6). STIM1 is proposed to exist as dimers in resting cells. In response to depletion of ER Ca^{2+}, STIM1 undergoes conformational changes that promote multimerization of the protein and translocation to specific ER-PM junctions, where the ER and PM are juxtaposed. At these sites, STIM1 accumulates as clusters, referred to as puncta, which in turn determine recruitment of Orai1 into the ER-PM junctions, resulting in STIM1-Orai1 interaction and activation of SOCE (1, 7, 8). Furthermore, these junctions also provide a platform for the assembly and recruitment of numerous proteins, including other ion channels [for example, transient receptor potential C1 (TRPC1) (9)]; CRAC channel regulators [for example, SARAF (10)]; cytoskeletal- and phosphatidylinositol 4,5-bisphosphate (PIP_2)-binding proteins [for example, septin (11)]; transcription factors [for example, NFAT (12)]; and enzymes [for example, adenylyl cyclase (13)]. Thus, assembly of Orai1 and STIM1 within the ER-PM junctions is associated with a SOCE-signaling complex that provides crucial short-term and long-term Ca^{2+} signals, which control such cellular activities as secretion, lymphocyte activation, gene expression, and growth.

STIM2 is a second ER-localized Ca^{2+}-sensor protein that has been associated with SOCE and Ca^{2+} signaling. It is ubiquitously expressed with STIM1 in human and mouse tissues as well as cell lines (14). Both STIM1 and STIM2 have a Ca^{2+}-binding EF-hand domain, a sterile alpha motif (SAM) domain, coiled-coiled (CC) domains, a STIM1 Orai1 activating region (SOAR), and a polybasic domain. However, the Ca^{2+} sensitivity and activation kinetics of STIM2 differ from those of STIM1 (15). Like STIM1, STIM2 is also mobilized in response to ER-Ca^{2+} store depletion. It clusters and translocates to form puncta in ER-PM junctions, where it has been reported to cluster with Orai1 and STIM1 (8, 16-18). However, STIM2 is a poor activator of Orai1 and SOCE as compared to STIM1. The key difference in efficiency of gating of Orai1 by the two STIM proteins has been narrowed down to Phe^{394} that is present in STIM1-SOAR domain, but not in STIM2-SOAR, as well as the relatively weaker interaction of STIM2-SOAR domain with Orai1 (8). Additionally, STIM1 puncta formation in the ER-PM junctions is triggered when ER-Ca^{2+} is relatively low, while STIM2 appears to form puncta with minimal depletion of ER-Ca^{2+}.

The distinct responses of STIM1 and STIM2 to ER-[Ca^{2+}] is likely to be physiologically important because relatively high levels of stimulation are required to substantially and globally deplete ER-Ca^{2+} stores, whereas low but physiologically relevant stimulus intensities induce less depletion (19). When compared with STIM1, the relatively lower Ca^{2+} affinity of the STIM2 EF-hand domain together with the kinetics of Ca^{2+} dissociation,

SAM domain stability, and the higher affinity of its polybasic domain for plasma membrane PIP_2, enables STIM2 to cluster at ER-PM junctions in response to minimal depletion of ER-Ca^{2+} stores (16, 20-24). Thus, STIM2 has been proposed to regulate Ca^{2+} entry in unstimulated cells for maintenance of cytosolic Ca^{2+} or to gate Orai1 at low concentrations of agonist stimulation (16, 25, 26). In addition, decreases in SOCE and SOCE-dependent gene expression have been reported following targeted genetic knockout of STIM2 in mouse T lymphocytes and fibroblasts, but not in vascular smooth muscle cells (27, 28).

We have examined the physiological role of STIM2 in agonist-induced Ca^{2+} signaling and SOCE. Neurotransmitter stimulation of muscarinic cholinergic receptors in salivary glands increases fluid secretion by inducing a sustained elevation of $[Ca^{2+}]_i$ that is primarily dependent on activation of SOCE in acinar cells. The spatial pattern of $[Ca^{2+}]_i$ increase as well as the amplitude are important in determining the maximal secretory response in salivary and pancreatic gland acinar cells (29). The SOCE-dependent increase in intracellular calcium concentration ($[Ca^{2+}]_i$) in salivary gland acinar cells regulates the activities of key ion channels that generate an osmotic gradient required to drive vectorial flow of water. STIM1 and Orai1 are necessary for agonist-dependent SOCE in these cells (30). In addition, TRPC1 also contributes to agonist stimulation of fluid secretion and $[Ca^{2+}]_i$ elevation following activation of SOCE, as shown by studies using $TRPC1^{-/-}$ mice (31, 32). TRPC1 is gated by STIM1 and is dependent on Orai1 for activation (9). Our previous studies have shown that TRPC1 clusters with Orai1 and STIM1 and that Orai1-mediated Ca^{2+} entry triggers the recruitment of TRPC1 into the plasma membrane. This results in amplification of the Ca^{2+} signal generated by Orai1-mediated Ca^{2+} entry (9, 31). Thus, Orai1-STIM1-mediated SOCE is critical in the regulation of Ca^{2+} signaling and the physiological function of acinar cells.

We found that STIM2 promotes STIM1 clustering in ER-PM junctions under conditions when there is less depletion of ER-Ca^{2+}, thus increasing assembly of the Orai1-STIM1 complex and activation of SOCE in response to stimulation of cells with pharmacological agonists of muscarinic acetylcholine receptors. We show that targeted knockout of STIM2 within salivary glands of $STIM2^{fl/fl}$ mice results in a reduction of fluid secretion at relatively low stimulus intensities. Furthermore, acinar cells isolated from glands following knockout of STIM2 display reduced $[Ca^{2+}]_i$ increases following stimulation with muscarinic receptor agonists. To understand the mechanism underlying the requirement for STIM2 in SOCE, we measured agonist-stimulated $[Ca^{2+}]_i$ changes and Ca^{2+}-dependent cell function in HEK293 cells. Our findings suggest that STIM2 recruits STIM1 and increases formation of STIM1 puncta in ER-PM junctions at low stimulus intensities and thus increases the agonist sensitivity of STIM1-Orai1 channel complex assembly and SOCE activation.

RESULTS

Knockout of STIM2 in mouse submandibular gland diminishes agonist-stimulated fluid secretion

We assessed the physiological relevance of STIM2 by measuring salivary fluid secretion activated is response to muscarinic cholinergic receptors in vivo in a mouse model. We used $STIM2^{fl/fl}$ mice to knockout STIM2 specifically in submandibular glands by in vivo delivery

of AdCRE-GFP by cannulation of their salivary gland excretory duct and tested the mice 7-10 days after viral delivery. Control STIM2$^{fl/fl}$ mice received Ad-GFP. When stimulated with pilocarpine (0.25 mg/kg body weight), the total volume and rate of saliva secretion was significantly reduced in STIM2$^{fl/fl}$ +Cre mice compared to the control group (Fig. 1, A and B). Remarkably, there was no significant difference in saliva secretion between the groups when mice were stimulated with higher amounts of pilocarpine (0.5 mg/kg body weight). Further, at either concentrations of pilocarpine, saliva flow and total volume produced was similar in control wild type (WT) and STIM2$^{fl/fl}$ mice.

Muscarinic receptor-dependent $[Ca^{2+}]_i$ increase was assessed in fura2-loaded acinar cells prepared from submandibular glands of STIM2$^{fl/fl}$+Cre mice and control mice following stimulation with increasing concentrations of the agonist, carbachol (CCh). In acinar cells from control mice, CCh induced a dose-dependent, sustained $[Ca^{2+}]_i$ elevation (reflected by the increase in 340/380nm fluorescence ratio shown in the figures). This sustained $[Ca^{2+}]_i$ elevation is critical for fluid secretion and is dependent on Ca^{2+} entry (29, 31, 32). In cells from STIM2$^{fl/fl}$+Cre mice stimulated with low concentrations of CCh, 300 nM and 1μM, (Fig.1C, D) the increase in $[Ca^{2+}]_i$ was transient and the amplitude was significantly reduced compared to the response in control cells. In contrast, at the highest concentration of CCh (100 μM), $[Ca^{2+}]_i$ increase was the same in cells prepared from control and STIM2-knockout glands. The recovery of function with the highest concentration of muscarinic agonist indicated that integrity of the glands was not compromised and the secretory capability of the acinar cells was unaffected by knockout of STIM2. Moreover, glands from STIM2$^{fl/fl}$ and STIM2$^{fl/fl}$+Cre mice were morphologically similar (fig. S1A). STIM2 abundance was specifically decreased in glands receiving AdCRE-GFP virus while STIM1, TRPC1, and Orai1 abundance was unaffected (fig. S1B). Thus, loss of STIM2 specifically diminished agonist-dependent saliva secretion in vivo and was associated with a reduction in agonist-stimulated $[Ca^{2+}]_i$ increase in dispersed acinar cells.

Knockdown of STIM2 in HEK293 cells reduces agonist-stimulated NFAT activation

Nuclear translocation of NFAT in HEK293 cells is dependent on SOCE-generated $[Ca^{2+}]_i$ increase mediated by the STIM1-Orai1 complex (9, 12, 33, 34). Activation of NFAT has been proposed to be an all-or-none event that is only triggered when local $[Ca^{2+}]_i$ near the Orai1 channel is raised above the threshold required for calmodulin-dependent activation of calcineurin (12, 34). Calcineurin dephosphorylates NFAT, which then moves from the cytosol to the nucleus where it regulates gene expression. Using siRNA, we knocked down STIM2 in HEK293 cells expressing green fluorescent protein (GFP)-tagged NFAT (GFP-NFAT). Knockdown of STIM2 diminished CCh-stimulated GFP-NFAT translocation into the nucleus (Fig. 1E). The proportion of cells displaying nuclear translocation of GFP-NFAT in response to stimulation with 1 or 100 μM CCh was significantly decreased in siSTIM2 cells as compared to that in control cells under the same conditions (Fig. 1F). To determine if the cells were still capable of mediating SOCE and inducing NFAT translocation, we exposed the cells to thapsigargin (Tg) to completely deplete the ER Ca^{2+} store. A similar proportion of STIM2 knockdown cells displayed GFP-tagged NFAT translocation as the control cells, suggesting that STIM2 was specifically important for the

function of the STIM1-Orai1 channel when ER-Ca^{2+} stores are not completely depleted (Fig. 1F).

STIM2 determines the amount of agonist stimulation needed for SOCE activation

To elucidate the contribution of STIM2 to SOCE mediated by STIM1-Orai1 channels, we examined the pattern of CCh-stimulated Ca^{2+} responses over a range of stimulus intensities in individual HEK293 cells (control cells and following knockdown of endogenous STIM2). We verified that the siRNA specifically and efficiently reduced the abundance of STIM2, without affecting the abundance of STIM1 or Orai1 (fig. S2A). To measure SOCE, we monitored $[Ca^{2+}]_i$ in fura2-loaded cells stimulated with CCh in Ca^{2+}-free medium that was subsequently replaced with medium containing Ca^{2+}. The increase in $[Ca^{2+}]_i$ (represented by the increase in 340/380nm fluorescence ratio) in Ca^{2+}-free medium represents intracellular Ca^{2+} release; the second peak in fura2 fluorescence in the Ca^{2+}-containing medium represents Ca^{2+} entry. Knockdown of STIM2 significantly reduced the Ca^{2+} influx component activated by 1 or 100 μM CCh, whereas the magnitude of the initial Ca^{2+} signal, representing release from internal stores, was unaffected (fig. S2, B-E). At the single-cell level, stimulation with various [CCh], in the presence of Ca^{2+} in the extracellular medium, produced different patterns of Ca^{2+} responses (Fig. 2). With increasing stimulus intensities (50 nM-1000 μM), the CCh-induced Ca^{2+} responses were variable, including very low or negligible responses, oscillations that returned to baseline between each peak (baseline oscillations) (Fig. 2A, fig. S3A,B), oscillations that returned to a plateau of $[Ca^{2+}]_i$ above the baseline (Fig. 2B), and a nonoscillating response that slowly decayed to a $[Ca^{2+}]_i$ greater than the baseline (elevated plateau) (Fig. 2C, D). Nonetheless, at each concentration of CCh, a majority of the cell population showed a distinctive response.

Similar to knockdown of Orai1 (33), knockdown of endogenous STIM1 eliminated the increases in $[Ca^{2+}]_i$ due to Ca^{2+} entry induced by CCh (fig. S3C, D). In contrast, knockdown of endogenous STIM2 induced changes in the pattern of Ca^{2+} responses at all concentrations of CCh tested (Fig. 2A-D), without affecting the initial increase in $[Ca^{2+}]_i$, representing CCh-stimulated intracellular Ca^{2+} release (insets in fig. S2B and D show the response in a single cell). Thus, the distinct patterns of the CCh-induced Ca^{2+} responses correlated with the effect of STIM2 on SOCE. In addition, STIM2 knockdown also significantly reduced the frequency of oscillations, but only at the lower concentrations of CCh. We calculated the baseline oscillations that occurred in the 300-600s time frame, which primarily depended on SOCE, in cells exposed to 300 nM CCh and found a 59% reduction in the number of oscillations following STIM2 knockdown compared with control cells (4.59±0.26 in siSTIM2 cells versus 10.48±0.39 in control cells; $P<0.05$, N = 120-180 cells from 5-6 separate experiments, Student's t-test); whereas at 1 μM CCh, the number of oscillations in a subpopulation of the cells with baseline oscillations was similar (11.10±0.52 in siSTIM2 cells versus 11.12±0.56 in control cells; $P<0.05$, N = 120-190 cells from 6 separate experiments, Student's t-test). At higher stimulus intensities (1-1000 μM CCh), the sustained increases in $[Ca^{2+}]_i$ were converted to oscillatory responses in cells in which STIM2 was knocked down (Fig. 2, B-D). At each concentration of CCh tested, the proportion of cells exhibiting low Ca^{2+} responses (baseline oscillations or no responses) was increased in siSTIM2 cells (Fig. 2, B-D, bar graphs on the right). Similar results were obtained with

another STIM2-specific siRNA (fig. S3E, F). Thus, at each [CCh], knockdown of endogenous STIM2 resulted in a change in the overall cellular responses to resemble those seen at the lower concentrations of CCh.

To determine if STIM2 affected the stimulus dependency of SOCE activation, we analyzed the dose response of CCh-induced $[Ca^{2+}]_i$ increase in control and STIM2-knockdown cells. We determined the increase in fura2 fluorescence ratio ($F-F_0$) at 300 s after CCh addition by averaging traces recorded in single cells (Fig. 2E). Representative average traces for a cell population stimulated with 300 nM and 100 μM are shown in fig. S3G, H. The $[Ca^{2+}]_i$ increase at 300 s after CCh addition was primarily due to SOCE, because the intracellular Ca^{2+} release component decayed to baseline less than 200 s after CCh addition in a Ca^{2+}-free media (insets in fig. S2B, D). Knockdown of STIM2 induced a right shift in the dose-response curve relative to that in control cells (Fig. 2E) indicating that the presence of STIM2 increased the apparent CCh sensitivity of SOCE activation, which was consistent with the increase in the apparent $K_{½}$ for CCh in the siSTIM2 cells and the decrease in the Hill coefficient (n_H). This decrease in the stimulus sensitivity of SOCE activation was also reflected by the reduction in the total number of cells displaying measurable changes in $[Ca^{2+}]_i$ at the lower concentrations of CCh. Whereas control cells typically displayed baseline oscillations at lower concentrations of CCh and elevated plateau responses at higher concentrations, siSTIM2 cells exhibited mixed responses with baseline oscillations in a large proportion of cells even at higher concentrations of CCh, with a corresponding decrease in the number of cells with an elevated plateau response (Fig. 2F, G). Together these data indicated that STIM2 reduces the amount of stimulus needed to activate SOCE.

STIM2 promotes the formation of STIM1 puncta in ER-PM junctions at low stimulus intensities

At the levels of stimulation that primarily produce oscillations in $[Ca^{2+}]_i$, the ER-Ca^{2+} stores are not as depleted as in cells where higher stimulations produce an elevated plateau response. Therefore, we predicted that there would be comparatively less clustering of STIM1 in ER-PM junctions at the lower levels of stimulation. Relatively few studies have described movement of STIM1 and puncta formation in response to low levels of agonist stimulation (12, 19, 35). Indeed, heterologously expressed YFP-STIM1 formed puncta only when cells were stimulated with 1 μM CCh in the absence of external Ca^{2+}, which prevented refilling of the ER Ca^{2+}store (19). In this study, we examined puncta formation of heterologously expressed STIM2, STIM1, or Orai1 that were tagged with fluorescent proteins (cyan fluorescence protein (CFP), yellow fluorescence protein (YFP), or Cherry) in CCh-stimulated HEK293 cells using total internal reflection fluorescence (TIRF) microscopy. Consistent with the previous report (19), we found that there was minimal clustering and puncta formation in YFP-STIM1-expressing cells in response to stimulation with 1 μM CCh (Fig. 3A), which produced $[Ca^{2+}]_i$ oscillations in majority of the cells (Fig. 2B). Increasing the stimulus to 100 μM CCh in the same cell resulted in robust time-dependent increase both in the number of puncta as well as the fluorescence intensity within each puncta (Fig. 3A, B). In contrast, cells expressing YFP-STIM2 had a few puncta prior to stimulation, which increased in number and fluorescence intensity in response to stimulation with 1 μM CCh and further increased when the concentration of CCh was increased to 100

μM (Fig. 3A, B). When YFP-STIM1 and CFP-STIM2 were coexpressed, there was some colocalization prior to stimulation (Fig. 3C). However, the number of puncta containing both proteins, as well as their individual fluorescence intensities within the puncta, increased at the lower stimulus intensity (1 μM CCh), and further increased when the [CCh] was raised to 100 μM (Fig. 3C-E). Quantitative analysis of the puncta fluorescence revealed that YFP-STIM1 extensively coclustered with CFP-STIM2 (Fig. 3C and E). Depletion of ER Ca^{2+} with Tg similarly induced coclustering of YFP-STIM1 and CFP-STIM2 in cells expressing both proteins (fig. S4A). We further confirmed that endogenous STIM1 and STIM2 also behaved similar to the heterologously expressed proteins following agonist stimulation of cells. CCh stimulation of HEK293 cells induced a dose-dependent increase in coimmunoprecipitation of endogenous STIM2 with STIM1 when compared to resting cells, (Fig. 3F). Together, our findings indicate that STIM2 associates with STIM1 and promotes STIM1 clustering and puncta formation in ER-PM junctions at low stimulus intensities when there is minimal depletion of the ER-Ca^{2+}.

STIM2-dependent clustering of STIM1 increases the assembly of STIM1-Orai1 channel complexes at low stimulus intensities

We next examined the effect of STIM2 on the recruitment of Orai1 to STIM1 puncta in ER-PM junctions. Heterologous expression of Orai1-CFP alone does not result in the formation of Orai1 clusters within the plasma membrane in response to ER Ca^{2+} depletion, even with maximal levels of stimulation (7, 36, 37); whereas, when coexpressed with STIM1, Orai1-CFP clusters in response to ER Ca^{2+} store depletion. Further, both proteins colocalize in puncta within ER-PM junctions, which have been identified as the site of SOCE (38). STIM1 clusters have been proposed to bind and trap Orai1 channels within these junctions (7). Additionally, Orai1 can recruit a STIM1 mutant lacking the C-terminal polybasic domain (STIM1ΔK, which does not form puncta on its own) to the cell periphery by binding to the SOAR domain of STIM1ΔK (7). Thus, we examined whether coexpression of Orai1-CFP promoted the formation of YFP-STIM1 puncta in cells stimulated with low levels of agonist. Unlike coexpression of CFP-STIM2 (Fig. 3C), coexpression of Orai1-CFP did not promote YFP-STIM1 puncta formation in response to 1 μM CCh, although coclusters of YFP-STIM1 with Orai1-CFP were abundant at 100 μM CCh (Fig. 4A). When YFP-STIM2 was expressed together with Orai1-CFP and Cherry-STIM1, all three proteins coclustered within puncta in cells exposed to 1 μM CCh, and this coclustering was increased in response to 100 μM CCh (Fig. 4B). Line scans below the images confirmed the colocalization of Orai1-CFP, Cherry-STIM1, and YFP-STIM2 within the same puncta. We also detected an increase in the individual fluorescence intensities of the three proteins in puncta in cells exposed to increasing concentrations of CCh (Fig. 4B). These data indicated that STIM2 enhanced the assembly of STIM1-Orai1 complexes by promoting STIM1 recruitment into puncta within ER-PM junctions under conditions that cause relatively little ER Ca^{2+} store depletion The EF-hand domain of STIM2 has a lower affinity for Ca^{2+}, compared to that of STIM1, which accounts for its ability to sense small depletions in ER Ca^{2+}. Mutation of three key residues in the EF-hand of STIM1 ($STIM1_{EF\rightarrow STIM2}$) decreases its affinity for Ca^{2+} to resemble that of STIM2 (16). Unlike wild-type YFP-STIM1, 1 μM CCh induced the clustering of YFP-$STIM1_{EF\rightarrow STIM2}$, which was increased with subsequent addition of 100

μM CCh (fig. S4B), suggesting that the inability of STIM1 to cluster at low levels of agonist stimulation is due to the higher Ca^{2+} affinity of its EF-hand domain.

The C-terminal polybasic domain of STIM2 is required for clustering of STIM1 in ER-PM junctions at low stimulus intensities

The polybasic domain, which is present in the C-terminus of both STIM proteins, has been suggested to bind to plasma membrane PIP_2 and contribute to the stabilization of STIM puncta in the ER-PM junctions (1, 7, 23, 24). A STIM1 mutant lacking the polybasic domain (aa 671-685, STIM1ΔK) fails to form puncta when expressed alone in cells even in response to stimulation (1). However, STIM1ΔK formed puncta following agonist stimulation when coexpressed with Orai1 (7). To assess the role of the polybasic domain in STIM2 in puncta formation, we created a mutant for YFP-STIM2 (STIM2ΔK5) that lacks the last 5 amino acids (aa 829-833) at the end of the polybasic domain. YFP-STIM2ΔK5 did not display puncta formation in response to ER Ca^{2+} store depletion by Tg when expressed alone or together with Orai1-CFP (Fig. 5, A and B). Unlike wild-type YFP-STIM2 (Fig. 3C), coexpression of YFP-STIM2ΔK5 with CFP-STIM1 did not promote formation of STIM1 puncta at low stimulus intensity (1 μM CCh) and neither did the STIM2 mutant cocluster with STIM1 in response to high level of stimulus (100 μM CCh) (Fig. 5C). Furthermore, when Orai1-CFP was coexpressed in cells together with Cherry-STIM1 and YFP-STIM2ΔK5, only Cherry-STIM1 and Orai1-CFP strongly coclustered and only at higher [CCh], while YFP-STIM2ΔK5 did not show clustering at either [CCh] (Fig. 5E).

To examine the effect of the STIM2ΔK5 on endogenous SOCE, we measured CCh-stimulated Ca^{2+} responses in cells expressing this STIM2 mutant. Similar to the effect seen in siSTIM2 cells (Fig. 2), expression of YFP-STIM2ΔK5 diminished and altered the pattern of $[Ca^{2+}]_i$ increases in single cells stimulated with either low (Fig. 5F) or high (Fig. 5G) levels of stimulus, consistent with a decrease in the agonist sensitivity of SOCE activation. These findings indicate that the polybasic domain of STIM2 plays a critical role in STIM1-Orai1 assembly and thus activation of SOCE at low stimulus intensities.

To further understand the molecular interactions involved in the recruitment of STIM1 by STIM2, we examined whether STIM1 polybasic domain is also required for the clustering of both STIM proteins. In contrast to STIM1, STIM1ΔK (mutant lacking the C-terminal polybasic domain), when expressed alone aggregated within the ER, but did not cluster and form puncta in the cell periphery in response to ER Ca^{2+} store depletion (7). However, when Orai1 was coexpressed STIM1ΔK, the two proteins coclustered in response to store depletion, and SOCE was activated (7). Consistent with this previous study (7), when Orai1-CFP and YFP-STIMΔK were coexpressed, they c-clustered and formed puncta when ER Ca^{2+} was depleted with Tg, whereas YFP-STIM1ΔK did not form puncta under these conditions when expressed alone (fig. S5, A and B). Coexpression of CFP-STIM2 with YFP-STIM1ΔK resulted in formation of puncta containing both STIM proteins in response to Tg (Fig. 6A). Additionally, we detected YFP-STIM1ΔK puncta both at low and high levels of stimulus in cells coexpressing CFP-STIM2 (Fig. 6B, C). These findings suggested that (i) STIM2 is sufficient to induce ER Ca^{2+} depletion-dependent STIM1 clustering; and

(ii) the association between STIM2 and STIM1 is dependent on the polybasic domain of STIM2.

DISCUSSION

The data revealed a role for STIM2 in modulating the agonist sensitivity of SOCE activation and Ca^{2+} signaling. We found that targeted knockout of STIM2 in exocrine salivary glands of $STIM2^{fl/fl}$ mice decreased fluid secretion in vivo following stimulation with relatively low concentrations of muscarinic cholinergic receptor agonist. Importantly, this decrease was associated with a reduction in the sustained $[Ca^{2+}]_i$ increase in acinar cells, the primary site of fluid secretion in salivary glands. This reduction in agonist-induced Ca^{2+} responses is also more pronounced at relatively lower levels of stimulus. Further analysis of agonist-induced Ca^{2+} signaling and clustering of STIM2, STIM1, and Orai1 at a single-cell level showed that STIM2 associated with and promoted STIM1 puncta formation in cells stimulated by low concentrations of agonist. Consequently, recruitment of Orai1 promoted the assembly of functional STIM1-Orai1 channel complexes within ER-PM junction, resulting in enhanced SOCE at low levels of stimulation. This effect of STIM2 at low concentrations of agonist, which are sufficient to produce a physiological effect, is especially relevant since there is less depletion of ER-Ca^{2+} stores and little STIM1 would be mobilized. Therefore, we suggested that STIM2, by promoting STIM1 clustering when ER-Ca^{2+} depletion is minimal, enhances the sensitivity and physiological response to agonist stimulation.

STIM1 and STIM2 vary in the Ca^{2+} affinities of their ER-luminal EF-hand domains (15, 16). Thus, STIM2, which has a lower affinity for Ca^{2+} than STIM1, can sense small decreases in the ER $[Ca^{2+}]$ and cluster at the ER-PM junction. Because STIM1 has a relatively higher affinity for Ca^{2+}, STIM1 would only cluster and localize to the ER-PM junction when the ER $[Ca^{2+}]$ is substantially depleted. Indeed, STIM1 does not form puncta at low stimulus intensities, when ER Ca^{2+} stores are minimally depleted (12, 19, 35). With TIRF microscopy and heterologously expressed fluorescent protein-tagged STIM2, STIM1, and Orai1, we showed that STIM2 promoted clustering of STIM1 and the formation of puncta in ER-PM junctions at relatively low stimulus intensities. Expressed alone, low levels of stimulation did not cluster STIM1, whereas in cells coexpressing STIM2 both proteins colocalized in puncta in response to stimulation with low concentrations of agonist. Further, mutations in the EF-hand domain of STIM1, which decrease the Ca^{2+} affinity to resemble that of STIM2, induced STIM1 clustering in response to stimulation with low concentrations of agonist, indicating that the Ca^{2+} affinity of the EF-hand domain is a primary determinant of the response to changes in ER $[Ca^{2+}]$. Similarly, when expressed together, Orai1, STIM1, and STIM2 coclustered in response to low amounts of stimulus. Nonetheless, our data indicated that STIM1 was the primary regulator of SOCE because loss of STIM1, but not STIM2, eliminated SOCE at all [CCh] tested. In contrast, loss of STIM2 altered the pattern of SOCE-dependent $[Ca^{2+}]_i$ increases: A sustained elevation in $[Ca^{2+}]_i$ commonly seen in cells stimulated at high concentrations of agonist was converted to a more oscillatory pattern of response, typically associated with lower stimulus intensity. Based on our data, we suggested that by enabling the assembly of functional STIM1-Orai1 channel complexes at low stimulus intensities, STIM2 enhances the agonist sensitivity of SOCE

activation. Indeed, knockdown of STIM2 had produced a 10-fold decrease in the apparent $K_{½}$ for SOCE induced by CCh and a significant decrease in the Hill coefficient values. It has been previously suggested that raising the concentration agonist increases the number of cells that display Ca^{2+} responses (34). We suggest that STIM2 is a key determinant of the SOCE response in a cell and contributes to the overall responsiveness of a cell population (that iis the proportion of cells that exhibit robust SOCE). Previous studies have shown that mouse T cells and fibroblasts lacking STIM2 display a decrease in SOCE, cytokine production, and nuclear translocation of the transcription factor NFAT. Interestingly, mice lacking both STIM2 and STIM1 develop autoimmune disease (27). Reduced protein expression of STIM2 impairs SOCE and Ca^{2+}-dependent gene expression, contributing to neuronal disease in mutant presenilin mice (39).

Based on our findings, we propose a model (Fig. 7) in which, prior to stimulation, STIM1 and STIM2 are diffusely localized within the ER and Orai1 is in the plasma membrane. To simplify the model, we have not displayed a dimer state for either STIM protein in resting (unstimulated) cells, although STIM1 may exist as a dimer in resting cells (40). According to our model, stimulation with low concentration of agonist induces minimal depletion of ER-Ca^{2+} stores. Because, compared to STIM1, STIM2 is more sensitive to small changes in the ER [Ca^{2+}]c, STIM2 is mobilized and clusters within ER-PM junctions. We hypothesize that because the domains involved in STIM1-STIM1 interactions, such as the SAM and the coiled-coil domains, are conserved in STIM2, STIM2 could interact with STIM1 through these domains to form heteromeric STIM1-STIM2 complexes that can be recruited to ER-PM junctions. Thus, in the model we show that STIM2 recruits STIM1 to these junctions when there is less ER-Ca^{2+} store depletion, conditions under which STIM1 cannot translocate on its own. Oligomerization of STIM1 is sufficient to drive puncta formation and activation of SOCE (41). Our study suggests that under conditions of minimal ER-Ca^{2+} store depletion STIM2 is a critical protein that determines STIM1 clustering and puncta formation in ER-PM junctions, thus enhancing recruitment and activation of Orai1, enabling SOCE necessary for regulation of cell function at relatively low stimulus intensities.

We presented two additional findings that further support our model. First, we showed that STIM2 promoted recruitment of STIM1ΔK into puncta, presumably representing ER-PM junctions. STIM1ΔK lacks its polybasic tail domain and cannot form puncta on its own. Additionally, we showed that the STIM2 polybasic domain is required for promoting STIM1 clustering and assembly of STIM1-Orai1 at low concentrations of agonist. Expression of a STIM2 mutant lacking the five C-terminal amino acid residues decreased STIM1 puncta formation as well as agonist-mediated stimulation of SOCE. The STIM2 polybasic domain has been predicted to have a stronger binding efficiency to plasma membrane PIP_2 than that of STIM1 (24). In vitro studies show that a dimer of STIM2 is sufficient for stable binding to the lipids, whereas a tetramer of STIM1 is required to achieve the same level of binding (24). We propose that at lower levels of stimulation, the STIM2 polybasic domain provides sufficient positive charges required for the interaction of the STIM2-STIM1 complex with $_{\text{the}}$ PM and promotes the clustering of both proteins within ER-PM junctions. In contrast, stimulation with higher concentrations of agonist results in greater depletion of the ER-Ca^{2+} stores with more STIM1 mobilization, promoting formation of STIM1-STIM1 homomers and assembly of additional STIM1-Orai1 channels (Fig. 7). Further studies will

be required to resolve protein stoichiometry of the STIM2-STIM1-Orai1 channel complex, as well as the exact sequence of events and molecular interactions between STIM2-STIM1 that are involved in recruitment of STIM1 to microdomains where SOCE occurs at low stimulus intensities.

Previous studies with lymphocytes have shown that STIM1 oligomerization is the primary event that drives STIM1 coupling to Orai1 and activation of SOCE. It has also been reported that STIM1 redistribution into ER-PM junctions and activation of I_{CRAC} have similar dependence on the ER $[Ca^{2+}]$ (41). Importantly, the similarity between STIM1 and I_{CRAC} dose-response curves indicates that the concentration of STIM1 at ER-PM junctions determines Orai1 clustering and activation. In contrast, STIM2 redistributes to ER-PM junctions at higher $[Ca^{2+}]_{ER}$ ($K_{½}$ = 406 μM) than STIM1 ($K_{½}$ = 210 μM) (16, 41). Our findings demonstrated that STIM2 associated with and promoted STIM1 puncta formation in the ER-PM junctions, enabling assembly of the STIM1-Orai1 complex and gating of Orai1 by STIM1. Our data showed that this function of STIM2 was especially relevant at low stimulus intensities when there is less ER-Ca^{2+} depletion and STIM1 is poorly clustered. Although STIM1 diffuses and moves freely within the ER membrane in unstimulated cells, ER-Ca^{2+} store depletion induces aggregation and immobilization of STIM1 in ER domains that are located in close proximity to the PM. It has been suggested that this stabilization of STIM1 aggregates is mediated by interaction of the polybasic domain (aa 671-685) with PIP_2 in the plasma membrane (1, 7, 24). The formation of STIM1 puncta drives recruitment of Orai1 into the same region resulting in interaction of the two proteins and gating of Orai1. The present study identified STIM2 as a physiologically relevant protein that recruited STIM1 to ER-PM junctions and promoted assembly of STIM1-Orai1 channel complexes, thereby tuning the agonist -sensitivity of Ca^{2+} signaling and cell function.

MATERIALS AND METHODS

Cell Culture, RNAi Transfection and Reagents

HEK293 cells were cultured in Dulbecco's MEM supplemented with 10% heat-inactivated fetal bovine serum, 1% glutamine and 1% penicillin/streptomycin. The siRNAs for human STIM1 (siSTIM1) were obtained from Dharmacon (Pittsburgh, PA), whereas that for human STIM2 (siSTIM2) were from Life Technologies (Grand Island, NY) and Dharmacon. Specificity of knockdown using siSTIM1 has been reported previously (9). Lipofectamine RNAiMAX (Life Technologies) was used for siRNA transfection alone, while Lipofectamine 2000 (Life Technologies) was used for all other transfections. Mock transfections of control cells were conducted using an empty vector or a scrambled siRNA. Cells were typically used 24-48h post-transfection. All other reagents used were of molecular biology grade obtained from Sigma-Aldrich (St Louis, MO) unless mentioned otherwise.

Constructs

YFP- and CFP-STIM1 (wild type; ΔK mutant) and YFP- and CFP-STIM2 were obtained from Tobias Meyer (Stanford University, Stanford, CA). Orai1-YFP and -CFP were

obtained from Tamas Balla (NIDCR, NIH, Bethesda, MD), whereas Cherry-STIM1 was from Richard Lewis (Stanford University, Stanford, CA). YFP-STIM1$_{EF\rightarrow STIM2}$ was obtained from Addgene (Cambridge, MA; plasmid 18865). YFP-STIM2ΔK5 was generated using the GeneArt® Site-Directed Mutagenesis System (Life Technologies) according to manufacturer's protocol. A STOP codon was introduced after amino 828 to eliminate the last 5aa within the polybasic domain. The resulting construct was then sequenced to confirm this deletion. The digested construct was purified using the Qiagen Gel Purification Kit (Qiagen, Valencia, CA) and subsequently ligated using the T4 DNA ligase (New England Biolabs, Ipswich, MA) as per manufacturer's instructions.

$[Ca^{2+}]_i$ Measurements

Fura2 fluorescence was measured in single HEK293 cells as described previously (42), using a Till Photonics Polychrome V spectrofluorimeter (FEI, Hillsboro, OR) and MetaFluor imaging software (Molecular Devices, Sunnyvale, CA) on an Olympus IX21 microscope (Olympus, Center Valley, PA). For dispersed acinar cells from mouse salivary glands, cells were incubated with 2 μM fura2-AM and allowed to attach to a glass-bottomed dish (MatTek Corp., Ashland, MA) for 30 min at 37°C in a 5% CO_2 incubator. Cells were selected based on their acinar-like morphology. Experiments were primarily done by stimulating cells with CCh in a Ca^{2+}-containing standard extracellular solution (SES; 145 mM NaCl, 5 mM KCl, 1 mM $MgCl_2$, 10 mM HEPES, 10 mM glucose, 1 mM $CaCl_2$, pH 7.4 (NaOH), (42)). For Ca^{2+} addback or extracellular Ca^{2+}-free experiments, cells were stimulated in SES without 1 mM $CaCl_2$ present in the buffer.

TIRF and confocal microscopy

TIRF microscopy was conducted using an Olympus IX81 motorized inverted microscope (Olympus) as described previously (42), using 447, 514, and 568 nm lasers for excitation of CFP, YFP, and Cherry, respectively; a TIRF-optimized Olympus Plan APO 60x (1.45 NA) oil immersion objective; and Lambda 10-3 filter wheel (Sutter Instruments, Novato, CA) containing 480-band pass (BP 40m), 525-band pass (BP 50m), and 605-band pass (BP 52m) filters for emission. Images were collected using a Q-Imaging Rolera e-mc^2 camera (Photometrics, Tucson, AZ) and the MetaMorph imaging software (Molecular Devices). MetaMorph was also used to measure the linescans and fluorescence intensities of puncta before and after stimulation with CCh. These values were then plotted using the Origin 8.6 software (OriginLab, Northampton, MA). Confocal microscopy was conducted using the FluoView FV1000 confocal scanning microscope system (Olympus). The images shown in the figures were of cells stimulated with the indicated [CCh] or [Tg] for 5-8 min in a Ca^{2+}-containing SES.

Western blotting

Cells were washed with 1X PBS and lysed in RIPA buffer supplemented with protease inhibitors (Thermo Fisher Scientific, Waltham, MA). The lysates were then centrifuged at 12,000×g for 30 min at 4°C, and the supernatant was collected analyzed by SDS-PAGE and Western blotting. Antibodies recognizing -STIM1 (Cell Signaling Technology, Danvers, MA), STIM2 (Cell Signaling Technology), Orai1 (GeneTex, Irvine, CA) or actin (Abcam, Cambridge, MA) were used at 1:1000 dilutions.

In vivo adenoviral vector delivery and saliva collection

The generation of STIM2$^{fl/fl}$ mice used in this study has been described previously (27). Mice were approximately 8 weeks of age at the time of experimentation. All experiments were executed under a protocol approved by the NIDCR Animal Care and Use Committee and were done in compliance with the Guide for the Care and Use of Laboratory Animal Resources National Research Council. The mean body weight of the mice used in this study was 27.3 ± 3.94 kg for control, 32.03 ± 2.28 kg for STIM2$^{fl/fl}$ and 26.75 ± 3.46 kg for STIM2$^{fl/fl}$+Cre. Mice were anesthetized by intramuscular injection with ketamine (60 mg/kg body weight) and xylazine (8 mg/kg body weight). The adenoviral vectors, AdControl or AdCre-GFP (at 5x10^9 particles/gland), were administered to both submandibular glands by retrograde ductal cannulation. Saliva collections were conducted 7-10 days post-transduction whereby anesthetized mice were stimulated by 0.25 or 0.5 mg/kg body weight of pilocarpine that was delivered subcutaneously. Whole saliva was collected with a 75 mm hematocrit tube (Drummond Scientific, Broomall, PA) into pre-weighed 1.5 ml Eppendorf tubes for 5, 10, and 30 min. The tubes were then re-weighed to calculate the volume of saliva collected.

Dispersion of salivary gland cells

Salivary glands were quickly excised from mice, trimmed of connective tissues, and finely minced (1 mm pieces) in a digestion medium (Eagle's Minimal Essential Medium, Life Technologies) containing 4kU of collagenase (Worthington, Lakewood, NJ) and 1% BSA. Cells were maintained at 37°C and thoroughly gassed with 95% O_2 and 5% CO_2 until used.

Morphological assessment of salivary glands

Salivary glands were fixed in 10% buffered formalin, embedded in paraffin, and then sectioned (5 μm thickness). The tissue sections were stained with hematoxylin and eosin (H&E), and then mounted in Permount. Stained sections were imaged using a Q-Imaging QICAM Fast1394 (Photometrics) camera and MetaMorph software (Molecular Devices) on an Olympus BX61 light microscope (Olympus).

Statistics

Data analyses were performed using Origin 8.6 (OriginLab) and GraphPad PRISM (GraphPad Software, La Jolla, CA). Statistical comparisons between two groups were made using the Student’s t-test, whereas comparisons of multiple groups were made using ANOVA followed by Sidak’s multiple comparisons test. The chi-square test was used to analyze responses in cell populations. Experimental values are expressed as mean ± SEM. Differences in the mean values were considered to be significant at $P<0.05$. Nonlinear curve fitting of the dose response curve was made using the Hill equation.

Supplementary Material

Refer to Web version on PubMed Central for supplementary material.

ACKNOWLEDGEMENTS

We thank Dr. Shmuel Muallem (MPTB, NIDCR, NIH) for his helpful discussions, Dr. Shyh-ing Jang (MPTB, NIDCR, NIH) for his technical assistance and Dr. Ilya Bezprozvanny (UT Southwestern, Dallas, TX) for his help in obtaining STIM2$^{fl/fl}$ mice. We would also like to thank Drs. Tobias Meyer and Richard Lewis (Stanford University, Stanford, CA), as well as Tamas Balla (NIDCR, NIH, Bethesda, MD) for kindly providing us the constructs used in this study (as listed in the Materials and Methods section). We thank Dr. Arthur Sherman (LBM, NIDDK, NIH) for his help in the statistical analyses.

Funding: We also acknowledge grant support from the NIDCR-DIR for ISA and from NIH (grant# AI097302) for SF.

REFERENCES

1. Liou J, Fivaz M, Inoue T, Meyer T. Live-cell imaging reveals sequential oligomerization and local plasma membrane targeting of stromal interaction molecule 1 after Ca^{2+} store depletion. Proc. Natl. Acad. Sci. USA. 2007; 104:9301. [PubMed: 17517596]
2. Muik M, Frischauf I, Derler I, Fahrner M, Bergsmann J, Eder P, Schindl R, Hesch C, Polzinger B, Fritsch R, Kahr H, Madl J, Gruber H, Groschner K, Romanin C. Dynamic coupling of the putative coiled-coil domain of ORAI1 with STIM1 mediates ORAI1 channel activation. J. Biol. Chem. 2008; 283:8014. [PubMed: 18187424]
3. Wu MM, Buchanan J, Luik RM, Lewis RS. Ca^{2+} store depletion causes STIM1 to accumulate in ER regions closely associated with the plasma membrane. J. Cell Biol. 2006; 174:803. [PubMed: 16966422]
4. Prakriya M, Feske S, Gwack Y, Srikanth S, Rao A, Hogan PG. Orai1 is an essential pore subunit of the CRAC channel. Nature. 2006; 443:230. [PubMed: 16921383]
5. Vig M, Peinelt C, Beck A, Koomoa DL, Rabah D, Koblan-Huberson M, Kraft S, Turner H, Fleig A, Penner R, Kinet JP. CRACM1 is a plasma membrane protein essential for store-operated Ca^{2+} entry. Science. 2006; 312:1220. [PubMed: 16645049]
6. Yeromin AV, Zhang SL, Jiang W, Yu Y, Safrina O, Cahalan MD. Molecular identification of the CRAC channel by altered ion selectivity in a mutant of Orai. Nature. 2006; 443:226. [PubMed: 16921385]
7. Park CY, Hoover PJ, Mullins FM, Bachhawat P, Covington ED, Raunser S, Walz T, Garcia KC, Dolmetsch RE, Lewis RS. STIM1 clusters and activates CRAC channels via direct binding of a cytosolic domain to Orai1. Cell. 2009; 136:876. [PubMed: 19249086]
8. Wang X, Wang Y, Zhou Y, Hendron E, Mancarella S, Andrake MD, Rothberg BS, Soboloff J, Gill DL. Distinct Orai-coupling domains in STIM1 and STIM2 define the Orai-activating site. Nat. Commun. 2014; 5:3183. [PubMed: 24492416]
9. Cheng KT, Liu X, Ong HL, Swaim W, Ambudkar IS. Local Ca^{2+} entry via Orai1 regulates plasma membrane recruitment of TRPC1 and controls cytosolic Ca^{2+} signals required for specific cell functions. PLoS Biol. 2011; 9:e1001025. [PubMed: 21408196]
10. Jha A, Ahuja M, Maleth J, Moreno CM, Yuan JP, Kim MS, Muallem S. The STIM1 CTID domain determines access of SARAF to SOAR to regulate Orai1 channel function. J. Cell Biol. 2013; 202:71. [PubMed: 23816623]
11. Sharma S, Quintana A, Findlay GM, Mettlen M, Baust B, Jain M, Nilsson R, Rao A, Hogan PG. An siRNA screen for NFAT activation identifies septins as coordinators of store-operated Ca^{2+} entry. Nature. 2013; 499:238. [PubMed: 23792561]
12. Kar P, Nelson C, Parekh AB. Selective Activation of the Transcription Factor NFAT1 by Calcium Microdomains near Ca^{2+} Release-activated Ca^{2+} (CRAC) Channels. J. Biol. Chem. 2011; 286:14795. [PubMed: 21325277]
13. Willoughby D, Everett KL, Halls ML, Pacheco J, Skroblin P, Vaca L, Klussmann E, Cooper DM. Direct binding between Orai1 and AC8 mediates dynamic interplay between Ca^{2+} and cAMP signaling. Sci. Signal. 2012; 5:ra29. [PubMed: 22494970]
14. Lopez E, Salido GM, Rosado JA, Berna-Erro A. Unraveling STIM2 function. J Physiol Biochem. 2012; 68:619. [PubMed: 22477146]

15. Stathopulos PB, Ikura M. Structural aspects of calcium-release activated calcium channel function. Channels (Austin). 2013; 7:344. [PubMed: 24213636]
16. Brandman O, Liou J, Park WS, Meyer T. STIM2 is a feedback regulator that stabilizes basal cytosolic and endoplasmic reticulum Ca^{2+} levels. Cell. 2007; 131:1327. [PubMed: 18160041]
17. Wang Y, Deng X, Zhou Y, Hendron E, Mancarella S, Ritchie MF, Tang XD, Baba Y, Kurosaki T, Mori Y, Soboloff J, Gill DL. STIM protein coupling in the activation of Orai channels. Proc. Natl. Acad. Sci. USA. 2009; 106:7391. [PubMed: 19376967]
18. Darbellay B, Arnaudeau S, Ceroni D, Bader CR, Konig S, Bernheim L. Human muscle economy myoblast differentiation and excitation-contraction coupling use the same molecular partners, STIM1 and STIM2. J. Biol. Chem. 2010; 285:22437. [PubMed: 20436167]
19. Ong HL, Liu X, Tsaneva-Atanasova K, Singh BB, Bandyopadhyay BC, Swaim WD, Russell JT, Hegde RS, Sherman A, Ambudkar IS. Relocalization of STIM1 for activation of store-operated Ca^{2+} entry is determined by the depletion of subplasma membrane endoplasmic reticulum Ca^{2+} store. J. Biol. Chem. 2007; 282:12176. [PubMed: 17298947]
20. Stathopulos PB, Zheng L, Ikura M. Stromal interaction molecule (STIM) 1 and STIM2 calcium sensing regions exhibit distinct unfolding and oligomerization kinetics. J. Biol. Chem. 2009; 284:728. [PubMed: 19019825]
21. Zheng L, Stathopulos PB, Li GY, Ikura M. Biophysical characterization of the EF-hand and SAM domain containing Ca^{2+} sensory region of STIM1 and STIM2. Biochem. Biophys. Res. Commun. 2008; 369:240. [PubMed: 18166150]
22. Zheng L, Stathopulos PB, Schindl R, Li GY, Romanin C, Ikura M. Auto-inhibitory role of the EF-SAM domain of STIM proteins in store-operated calcium entry. Proc. Natl. Acad. Sci. USA. 2011; 108:1337. [PubMed: 21217057]
23. Ercan E, Momburg F, Engel U, Temmerman K, Nickel W, Seedorf M. A conserved, lipid-mediated sorting mechanism of yeast Ist2 and mammalian STIM proteins to the peripheral ER. Traffic. 2009; 10:1802. [PubMed: 19845919]
24. Bhardwaj R, Muller HM, Nickel W, Seedorf M. Oligomerization and Ca^{2+}/calmodulin control binding of the ER Ca^{2+}-sensors STIM1 and STIM2 to plasma membrane lipids. Biosci. Rep. 2013; 33:e00077. [PubMed: 24044355]
25. Kar P, Bakowski D, Di Capite J, Nelson C, Parekh AB. Different agonists recruit different stromal interaction molecule proteins to support cytoplasmic Ca^{2+} oscillations and gene expression. Proc. Natl. Acad. Sci. USA. 2012; 109:6969. [PubMed: 22509043]
26. Thiel M, Lis A, Penner R. STIM2 drives Ca^{2+} oscillations through store-operated Ca^{2+} entry caused by mild store depletion. J. Physiol. 2013; 591:1433. [PubMed: 23359669]
27. Oh-Hora M, Yamashita M, Hogan PG, Sharma S, Lamperti E, Chung W, Prakriya M, Feske S, Rao A. Dual functions for the endoplasmic reticulum calcium sensors STIM1 and STIM2 in T cell activation and tolerance. Nat. Immunol. 2008; 9:432. [PubMed: 18327260]
28. Song MY, Makino A, Yuan JX. STIM2 Contributes to Enhanced Store-operated Ca Entry in Pulmonary Artery Smooth Muscle Cells from Patients with Idiopathic Pulmonary Arterial Hypertension. Pulm Circ. 2011; 1:84. [PubMed: 21709766]
29. Palk L, Sneyd J, Patterson K, Shuttleworth TJ, Yule DI, Maclaren O, Crampin EJ. Modelling the effects of calcium waves and oscillations on saliva secretion. J. Theor. Biol. 2012; 305:45. [PubMed: 22521411]
30. Ambudkar IS. Polarization of calcium signaling and fluid secretion in salivary gland cells. Curr. Med. Chem. 2012; 19:5774. [PubMed: 23061636]
31. Liu X, Cheng KT, Bandyopadhyay BC, Pani B, Dietrich A, Paria BC, Swaim WD, Beech D, Yildrim E, Singh BB, Birnbaumer L, Ambudkar IS. Attenuation of store-operated Ca^{2+} current impairs salivary gland fluid secretion in $TRPC1^{-/-}$ mice. Proc. Natl. Acad. Sci. USA. 2007; 104:17542. [PubMed: 17956991]
32. Hong JH, Li Q, Kim MS, Shin DM, Feske S, Birnbaumer L, Cheng KT, Ambudkar IS, Muallem S. Polarized but differential localization and recruitment of STIM1, Orai1 and TRPC channels in secretory cells. Traffic. 2011; 12:232. [PubMed: 21054717]

33. Ong HL, Jang SI, Ambudkar IS. Distinct contributions of Orai1 and TRPC1 to agonist-induced $[Ca^{2+}]_i$ signals determine specificity of Ca^{2+}-dependent gene expression. PLoS One. 2012; 7:e47146. [PubMed: 23115638]
34. Kar P, Nelson C, Parekh AB. CRAC channels drive digital activation and provide analog control and synergy to Ca^{2+}-dependent gene regulation. Curr. Biol. 2012; 22:242. [PubMed: 22245003]
35. Bird GS, Hwang SY, Smyth JT, Fukushima M, Boyles RR, Putney JW Jr. STIM1 is a calcium sensor specialized for digital signaling. Curr. Biol. 2009; 19:1724. [PubMed: 19765994]
36. Navarro-Borelly L, Somasundaram A, Yamashita M, Ren D, Miller RJ, Prakriya M. STIM1-Orai1 interactions and Orai1 conformational changes revealed by live-cell FRET microscopy. J. Physiol. 2008; 586:5383. [PubMed: 18832420]
37. Xu P, Lu J, Li Z, Yu X, Chen L, Xu T. Aggregation of STIM1 underneath the plasma membrane induces clustering of Orai1. Biochem. Biophys. Res. Commun. 2006; 350:969. [PubMed: 17045966]
38. Luik RM, Wu MM, Buchanan J, Lewis RS. The elementary unit of store-operated Ca^{2+} entry: local activation of CRAC channels by STIM1 at ER-plasma membrane junctions. J. Cell Biol. 2006; 174:815. [PubMed: 16966423]
39. Sun S, Zhang H, Liu J, Popugaeva E, Xu NJ, Feske S, White CL 3rd, Bezprozvanny I. Reduced Synaptic STIM2 Expression and Impaired Store-Operated Calcium Entry Cause Destabilization of Mature Spines in Mutant Presenilin Mice. Neuron. 2014; 82:79. [PubMed: 24698269]
40. Covington ED, Wu MM, Lewis RS. Essential role for the CRAC activation domain in store-dependent oligomerization of STIM1. Mol. Biol. Cell. 2010; 21:1897. [PubMed: 20375143]
41. Luik RM, Wang B, Prakriya M, Wu MM, Lewis RS. Oligomerization of STIM1 couples ER calcium depletion to CRAC channel activation. Nature. 2008; 454:538. [PubMed: 18596693]
42. Ong HL, Cheng KT, Liu X, Bandyopadhyay BC, Paria BC, Soboloff J, Pani B, Gwack Y, Srikanth S, Singh BB, Gill DL, Ambudkar IS. Dynamic assembly of TRPC1-STIM1-Orai1 ternary complex is involved in store-operated calcium influx. Evidence for similarities in store-operated and calcium release-activated calcium channel components. J. Biol. Chem. 2007; 282:9105.

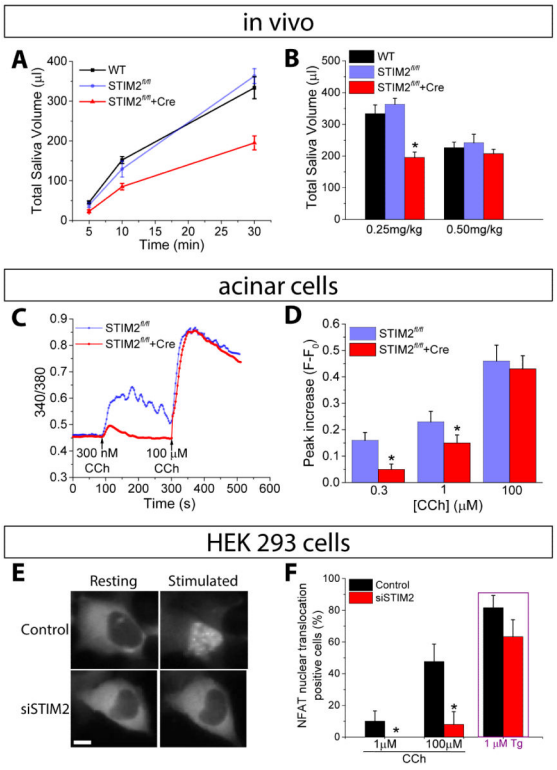

FIGURE 1. Targeted knockout of STIM2 in mouse salivary glands

(A) Saliva secretion following stimulation with pilocarpine (0.25 mg/kg body weight) in wild-type (WT), STIM2$^{fl/fl}$, and STIM2$^{fl/fl}$+Cre mice. (B) Bar graph showing total saliva collected after 30 min with the indicated amounts of pilocarpine [*P< 0.05, N = 9 or more mice per group; ANOVA was used to compare the saliva volume for STIM2$^{fl/fl}$, and STIM2$^{fl/fl}$+Cre mice with the WT mice]. (C and D) Representative traces showing changes in fura2 fluorescence following CCh stimulation of dispersed salivary gland acinar cells. Data are representative of 3 or more independent cell preparations, with 15-25 acini imaged per experiment. Each cell preparation used salivary glands from one mouse. (D) Peak increase in fura2 fluorescence (F - F_0), calculated using data from three different cell preparations [at each [CCh] [*P< 0.05, N = 72-77 cells from 3 different preparations; compared to the respective value for STIM2$^{fl/fl}$ using Student's t-test]. (E) Nuclear translocation of GFP-NFAT in control and siSTIM2-treated HEK293 cells, following stimulation with CCh or Tg. The images shown are representative of results obtained with 30-40 cells per experiments from 3 independent experiments. (F) Proportion (%) of cells showing nuclear translocation of GFP-NFAT at 25 min after the addition of the indicated concentrations of CCh or 10 min after the addition of 1 µM Tg [*P< 0.05, N = 100-110 cells per group from 3 separate experiments; chi-square test was used to compare nuclear translocation of GFP-NFAT between control and siSTIM2 cells at each stimulation.

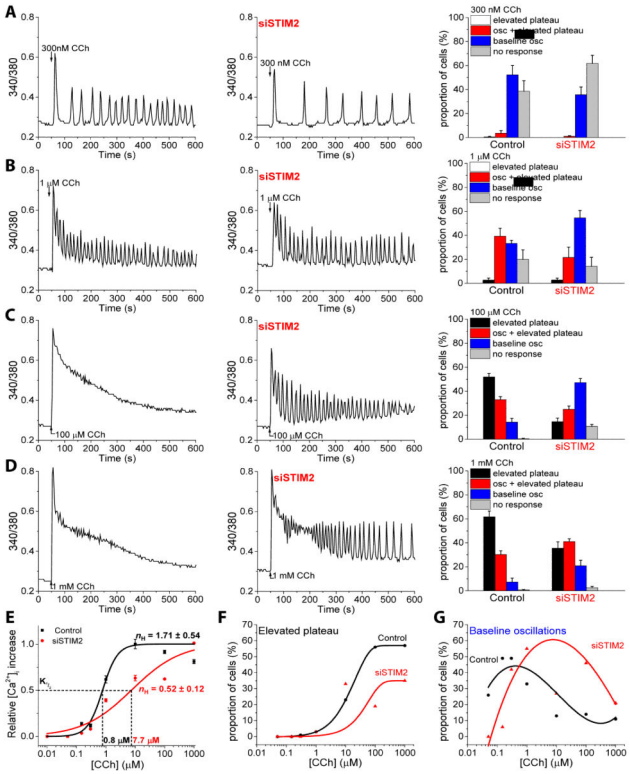

FIGURE 2. Modulation of CCh-induced Ca^{2+} responses by STIM2

(A-D) Fura2 fluorescence was monitored in control and siSTIM2-treated HEK293 cells stimulated with the indicated concentrations of CCh. Traces are representative of the type of response exhibited by the majority of cells at each [CCh] in control (left trace) and siSTIM2 (right trace) cells [N = at least 70 cells for each [CCh] in each of the 3 or more independent experiments]. The bar graphs show the proportion (%) of the cell population displaying various patterns of $[Ca^{2+}]_i$ changes at each [CCh]. Overall pattern of responses in siSTIM2 cells were significantly different from that in control cells at each [CCh] ($P<0.05$, N = 400-600 cells from 4-6 experiments; chi-square test). (E) Dose response curves showing the relative increases in $[Ca^{2+}]_i$ over baseline for each [CCh] ranging from 50 nM-1000 μM in control and siSTIM2 cells. (F) Proportion of the cells showing the elevated plateau response at each [CCh] in control and siSTIM2 cells. (G) Proportion of the cells showing baseline Ca^{2+}oscillations at each [CCh] in control and siSTIM2 cells. For (F) and (G), the N values are the same as in (A-D).

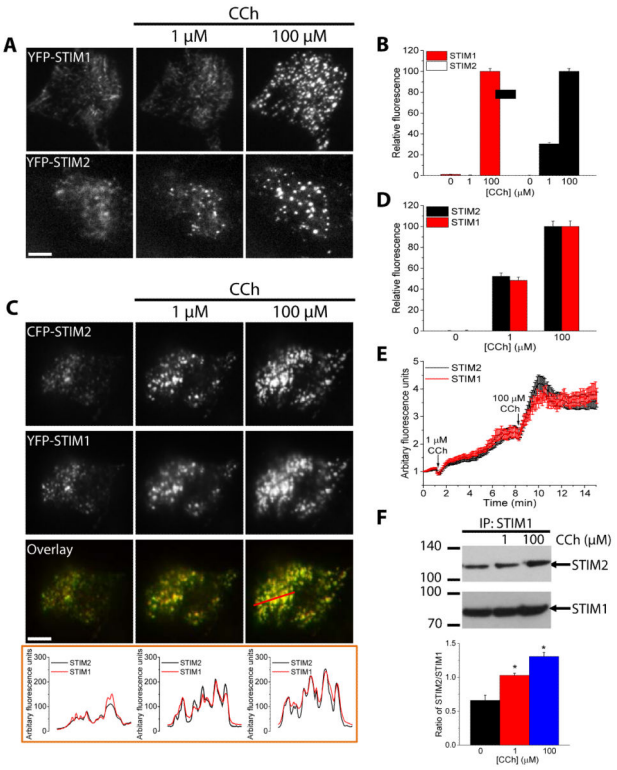

FIGURE 3. Clustering of STIM1 and STIM2 in response to relatively low and high levels of stimulation

Fluorescent tagged proteins were expressed, individually or together, in HEK293 cells. Cells were stimulated with the indicated concentrations of CCh and TIRF microscopy was used to image the fluorescence and visualize puncta in ER-PM junctions. The bar in this and subsequent figures indicates a scale of 10 μm. (A) Pattern of YFP-STIM1 (upper) and YFP-STIM2 (lower) fluorescence in cells individually expressing each construct sequentially stimulated with 1 and 100 μM CCh. (B) Bar graph showing representative changes in puncta fluorescence intensity for YFP-STIM1 and YFP-STIM2 at each [CCh], relative to the fluorescence at 100 μM CCh for each protein. A region of interest (ROI) was drawn around each puncta to quantify the changes in the fluorescence of individual puncta following each stimulation [N = 15-20 ROIs from each cell with 4-6 cells analyzed per experiment and with 3 or more separate experiments performed]. (C) Pattern of CFP-STIM2 (upper) and YFP-STIM1 (middle) fluorescence and the merged fluorescence (overlay in lower) in a cell co-expressing both proteins sequentially stimulated with 1 and 100 μM CCh. The graphs below the images show linescan measurements with the linescan region indicated in the rightmost image. (D) Bar graph showing relative increase in puncta fluorescence intensity for YFP-STIM1 and CFP-STIM2 following each stimulation in cells co-expressing both proteins [data are from 3 cells (average of 15-20 ROIs per cell) and is representative of 10-15 cells from 3 or more separate experiments performed]. (E) The time-dependent increase in co-expressed YFP-STIM1 and CFP-STIM2 fluorescence following stimulation with 1 and 100 μM CCh [ROIs and number of cells and experiments as described in (D)]. (F) Coimmunoprecipitation of endogenous STIM2 with endogenous STIM1 following stimulation with 1 and 100 μM CCh. The bar graph below the blot shows the abundance of

STIM2 relative to STIM1 in the immunoprecipitates at each [CCh] [*P<0.05, N = 3 or more separate experiments; ANOVA with Sidak's multiple comparisons test].

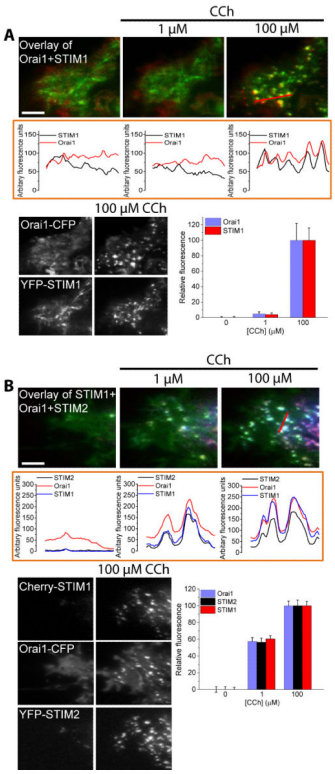

FIGURE 4. Clustering of fluorescent protein-tagged STIM1, STIM2, and Orai1 in response to relatively low and high levels of stimulation

Fluorescent tagged proteins were expressed, individually or together, in HEK293 cells that were stimulated with the indicated concentrations of CCh. TIRF microscopy was used to image the fluorescence and visualize puncta in ER-PM junctions. (A) Cells co-expressing YFP-STIM1 and Orai1-CFP were sequentially stimulated with 1 and 100 μM CCh. The merged fluorescence (overlay of images) of both proteins is shown in the upper panels, with the line scans immediately below each image for each [CCh] (the linescan region is indicated in the rightmost panel). Individual images showing the clustering or YFP-STIM1 and Orai1-CFP following stimulation with 100 μM CCh are below the linescans. The bar graph shows puncta fluorescence intensity (arbitrary units) for YFP-STIM1 and Orai1-CFP in cells stimulated with CCh, relative to that at 100 μM CCh (set at 100%). Data are from 4-6 cells (15-20 ROIs per cell) and are representative of results obtained in 3 or more independent experiments. (B) Cells co-expressing Cherry-STIM1, YFP-STIM2, and Orai1-CFP were sequentially stimulated with 1 and 100 μM CCh. The merged fluorescence (overlay) of all proteins is shown in the upper panels, with the line scans immediately below each image for each [CCh] (the region of the scan is indicated in the rightmost panel). Individual images show the clustering or Cherry STIM1, YFP-STIM2 and Orai1-CFP following stimulation with 100 μM CCh are shown below the linescans. The bar graph shows puncta fluorescence intensity (arbitrary units) for Cherry-STIM1, YFP-STIM2, and Orai1-CFP in cells stimulated with each [CCh] [fluorescence intensity at 100 μM CCh was set as 100% for each protein; N = 15-20 ROIs from each cell with 2-4 cells analyzed per experiment and with 3 or more separate experiments performed].

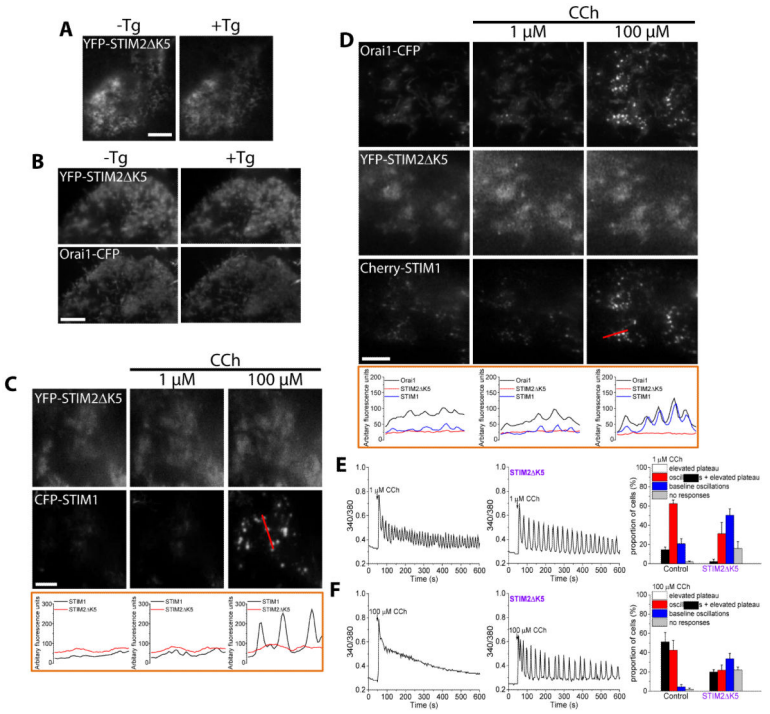

FIGURE 5. Effect of the STIM2ΔK5 mutant on CCh-induced STIM1 and Orai1 clustering and SOCE

Fluorescent tagged proteins were expressed, individually or together, in HEK293 cells that were stimulated with the indicated concentrations of CCh. TIRF microscopy was used to image the fluorescence and visualize puncta in ER-PM junctions. (A) Fluorescence of cells expressing YFP-STIM2ΔK5 alone in the presence or absence of thapsigargin (Tg, 1 μM for 5 min) to deplete ER Ca^{2+} stores. (B) Fluorescence of cells co-expressing YFP-STIM2ΔK5 and Orai1-CFP in the presence or absence of thapsigargin (Tg, 1 μM for 5 min). (C) Fluorescence of cells co-expressing YFP-STIM2ΔK5 and CFP-STIM1 following sequential stimulation with the indicated concentrations of CCh. The linescans are shown immediately below each image for each [CCh] (the linescan region is indicated in the rightmost panel). (*D)* Fluorescence of HEK293 cells co-expressing YFP-STIM2ΔK5, Cherry-STIM1, and Orai1-CFP following sequential stimulation with the indicated concentrations of CCh. The line scans are shown immediately below each image for each [CCh] (the linescan region is indicated in the rightmost panel). Images are representative of results obtained in 15-20 cells from at least 4 independent experiments. (E and F) Fluorescence traces representing Ca^{2+} responses exhibited by the majority of control cells (left) and HEK293 cells expressing STIM2ΔK5 (right) following stimulation with 1 (E) and 100 (F) μM CCh. Bar graphs show the percentage (%) of cells showing a given pattern of Ca^{2+}responses at each concentration of CCh. Overall pattern of responses in the two groups was significantly different [*P<0.05, N = 170-240 cells per group from 3-5 separate experiments; chi-square test].

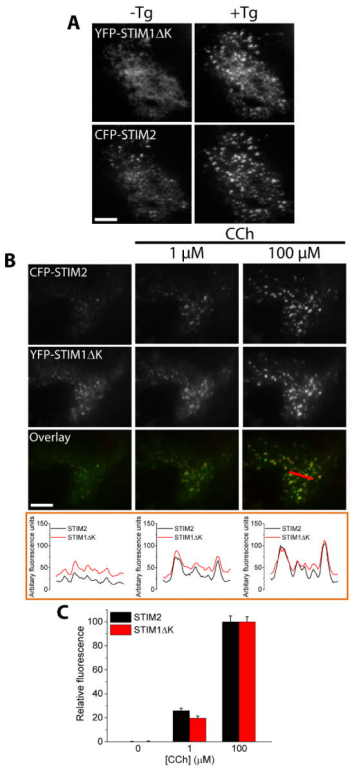

FIGURE 6. Effect of the STIM1ΔK mutant on CCh-induced STIM2 clustering

Fluorescent tagged proteins were expressed, individually or together, in HEK293 cells and TIRF microscopy was used to image the fluorescence and visualize puncta in ER-PM junctions. (A) Fluorescence of cells expressing YFP-STIM1ΔK and CFP-STIM2 in the presence or absence of thapsigargin (Tg, 1 μM for 5 min) to deplete ER Ca^{2+} stores. (B) Fluorescence of cells co-expressing YFP-STIM1ΔK and CFP-STIM2 following sequential stimulation with the indicated concentrations of CCh. The merged fluorescence (overlay) of all proteins is shown in the upper panels, with the linescans immediately below each image for each [CCh] (the linescan region is indicated in the rightmost panel). (C) The bar graph shows the changes in puncta fluorescence intensity for YFP-STIM1ΔK and CFP-STIM2 following each stimulation in cells co-expressing both proteins, relative to the intensity at 100 μM CCh. ROI was drawn around each puncta to quantify the changes in the fluorescence of individual proteins within the puncta following each stimulation [N = 15-20 ROIs from each cell with 2-4 cells analyzed per experiment and with 3 or more separate experiments performed].

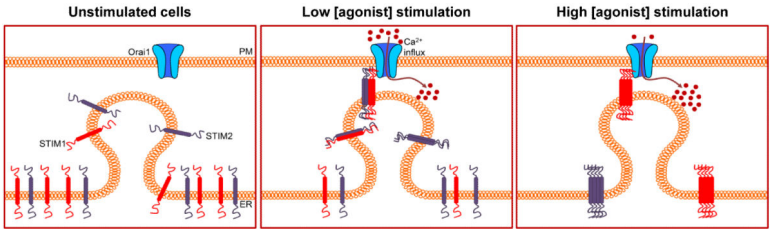

FIGURE 7. Model depicting the role of STIM2 in the clustering of STIM1 and activation of SOCE following intracellular Ca^{2+}-store depletion

In unstimulated cells, ER [Ca^{2+}] is high (blue) and the STIM proteins reside and are diffusively distributed in the ER membrane. Stimulation with relatively low concentration of agonist results in minimal depletion of the ER-Ca^{2+} stores and mobilization of STIM2. These conditions promote the formation of STIM2-STIM1 heteromers, which translocate to the ER-PM junctions where STIM1 interacts with Orai1 and activates SOCE. Substantial depletion of the ER-Ca^{2+} stores following stimulation with high concentrations of agonist drives the formation of STIM1 homomers and their recruitment to the ER-PM junctions where STIM1 activates Orai1. Because both STIM2-STIM1 heteromers and STIM1 homomers would form in response to high concentrations of agonist, we predict that Ca^{2+} influx would be greater than at the lower levels of stimulation.